IRIS AperTO

UNIVERSITÀ DEGLI STUDI DI TORINO

AperTO - Archivio Istituzionale Open Access dell'Università di Torino

Tracing the history of past treatments: A multi-analytical study of a 16th-century panel painting copy after Raphael

This is a pre print version of the following article:

Original Citation:

Availability:

This version is available http://hdl.handle.net/2318/2061910 since 2025-03-08T22:47:11Z

Published version:

DOI:10.1016/j.culher.2023.11.010

Terms of use:

Open Access

Anyone can freely access the full text of works made available as "Open Access". Works made available under a Creative Commons license can be used according to the terms and conditions of said license. Use of all other works requires consent of the right holder (author or publisher) if not exempted from copyright protection by the applicable law.

(Article begins on next page)

21 November 2026

Tracing the history of past treatments: a multi-analytical study of a 16th-century panel painting copy after Raphael

Tiziana Cavaleri [a,b]*, Claudia Pelosi[b], Claudia Caliri[c], Paolo Francesco Romano[c], Claudia Colantonio[b], Luca Lanteri[b], Giuseppe Calabrò[b], Anna Piccirillo[a], Bernadette Ventura[a], Stefania De Blasi[a], Chiara Riedo[d] & Dominique Scalarone[d]

[a] Centro per la Conservazione ed il Restauro dei Beni Culturali "La Venaria Reale" (CCR), via XX Settembre 18, 10078 Venaria Reale, Turin, Italy

[b] Department of Economy, Engineering, Society, and Business Organization (DEIM), University of Tuscia, Via del Paradiso 47, 01100 Viterbo, Italy

[c] Istituto di Scienze del Patrimonio Culturale, Consiglio Nazionale delle Ricerche (ISPC-CNR), Via Biblioteca 4, 95124 Catania, Italy

[d] Department of Chemistry, University of Turin, Via Pietro Giuria 7, 10125 Turin, Italy

* Corresponding author: tiziana.cavaleri@ccrvenaria.it

Abstract

A multi-analytical investigation and ad hoc sampling method designed to support the conservation treatment of a 16th-century panel painting are described in this work.

The painting, titled *Madonna of the Tent* and owned by the Musei Reali Torino (MRT, Turin, Italy), had been historically attributed to Raffaello Sanzio and subsequently identified as a copy after the Master – the original version of which is displayed at the Alte Pinakothek in Munich (Germany). The conservation treatment was carried out at Centro per la Conservazione ed il Restauro dei Beni Culturali "La Venaria Reale" (CCR), located in Venaria Reale (Turin, Italy): before treatment , the painted surface was particularly opaque and yellowed, suggesting the presence of different overlaying varnishes and, likely, overpainting.

The scientific study of this work had two main aims: knowing the exact number and composition of the overlaying varnishes – to select the best cleaning solution – and detecting the possible presence of overpainting. Therefore, understanding the original material and stratigraphy of the painting was propaedeutic to these aims. Coupling macro X-ray fluorescence scanning (MA-XRF), hypercolorimetric multispectral imaging (HMI), and UV-Vis-NIR fiber optic reflectance spectroscopy (FORS) allowed for general mapping and characterization of color paints and pigments. Observing and analyzing some cross sections with an optical microscope under Vis and UV light and SEM/EDS was essential for understanding the stratigraphy. An accurate study of the chemical composition of the varnishes and their position in the stratigraphy required an ad hoc sampling method and further micro-invasive analyses. Especially the image of a cross section under UV light was a guide to selectively remove the scrapings for Fourier transform infrared spectroscopy (FTIR) and pyrolysis-gas chromatography/mass spectrometry (Py-GC/MS) analyses. Based on perceptible differences in UV fluorescence of the layers, sampling of the varnishes was carried out, layer by layer, under a UV lamp. This work describes the complex process necessary to answer crucial questions in the conservation field, by exploiting both the complementarity and analogies between imaging and spot techniques. The outcomes and methodological approach enabled us to reconstruct the history of the past treatments and support the recent conservation treatment of the painting.

Keywords

Sampling method; methodological approach; multi-layered varnishes; pyrolysis-gas chromatography/mass spectrometry (Py-GC/MS); UV-induced visible luminescence (UVL); macro X-ray fluorescence (MA-XRF); hypercolorimetric multispectral imaging (HMI); fiber optic reflectance spectroscopy (FORS).

1. Introduction

The design and application of scientific analysis to support the conservation treatment of cultural heritage are fortunately becoming a widespread practice. The problems that may arise during a conservation treatment can be multiple and complex, but, in most cases, they imply a multi-analytical approach and the synergy of numerous professionals. The multi-analytical approach exploits the complementarity of analytical techniques to provide more coherent data on artistic materials and techniques. The interdisciplinary team favors the exchange of skills which is the basis for the development of new analytical techniques and research topics [1-12]. Not surprisingly, technological development in heritage science is moving in the direction of pushing the combination of two or more techniques in a single investigation [13-18]. Moreover, within this multidisciplinary setting, imaging and mapping technologies have developed rapidly compared to spot techniques: they are far more easily readable and communicable in a wider context [19-25].

The conservation treatment of a 16th-century panel painting carried out in the years 2018-2020 at Centro per la Conservazione ed il Restauro dei Beni Culturali "La Venaria Reale" (CCR) located in Venaria Reale (province of Turin, Italy) was the opportunity to test a methodological approach based on multi-analytical investigation and an ad hoc sampling method designed to support the conservation treatment of a very complex case study. The painting, titled *Madonna of the Tent* and owned by the Musei Reali Torino (MRT, Turin, Italy), had been historically attributed to Raffaello Sanzio and subsequently recognized as a 16th-century copy after the Master – the original version of which is displayed at the Alte Pinakothek in Munich, Germany [1, 26]. Interestingly, the back surface features a centimetric hollow engraved in the wood and an inscription reporting the following words: “Quadro del Divino Rafaele Sanzio/ D’Urbino”. Before the conservation treatment, the painted surface was particularly opaque and yellowed, suggesting the presence of different overlaying varnishes and, likely, overpainting.

The scientific study of the painting was handled by the CCR team with the valuable collaboration of various Universities and Research Institutions.

2. Research aim

Analyses and the methodological approach described in this paper were designed to answer two main questions that arose during the conservation treatment: detecting any possible overpainting and knowing the exact number and composition of the overlaying varnishes .

For the first aim, scanning macro X-ray fluorescence (MA-XRF), hypercolorimetric multispectral imaging (HMI), and UV-Vis-NIR fiber optic reflectance spectroscopy (UV-Vis-NIR FORS) were applied. Based on their complementarity, it was possible to investigate the original palette and map the overpainting. Then, some multi-layered samples were removed from the painting and prepared as cross sections to understand and compare the work’s stratigraphy on different points.

As for the second aim, d etecting different varnish layers required an in-depth analysis of the organic compounds layer by layer. This is a very challenging task due to both the complexity of the composition of natural resin and synthetic varnishes and the reduced thickness of the varnish layers. In this regard, some pioneering works reported the use of time-of-flight secondary ion mass spectrometry (ToF-SIMS) imaging to study paint cross sections and to identify simultaneously mineral pigments and organic components like binders and varnishes. The technique provides sub-micrometer resolution mass spectrometry images and high mass resolution, but the instrumentation is expensive and still not widely available. Moreover, sample preparation requires great care, and setting up the analytical conditions and data interpretation are very difficult, especially when mixtures of different organic substances are analyzed [27, 28]. Therefore, to shed light on the composition of the various varnish layers of the painting *Madonna of the Tent*, we preferred to rely on a separation technique with a high response specificity such as pyrolysis-gas chromatography/mass spectrometry (Py-GC/MS), complemented by Fourier transform infrared spectroscopy (FTIR) on selective samples. An ad hoc sampling method was designed for this scope.

3. Materials and methods

2.1 The case study of the Madonna of the Tent panel painting in Turin

The panel painting, titled *Madonna of the Tent* (Inv. 271, MRT, Turin, Italy), depicts the Virgin and Child with Saint John. Dimensions of the panel are 79 × 56 cm. As mentioned, a centimetric hollow and an inscription attesting to Raphael's manufacturing are on the back surface, the nature of which has already been studied [1, 26].

When arriving at CCR in Venaria Reale for the conservation treatment, the work showed a yellowed aspect that suggested the presence of several overlaying varnishes and, likely, overpainting. The painting technique appeared inhomogeneous with very full-bodied brushstrokes in some areas, as in the Virgin's blue mantle and the clouds, and much thinner and delicate brushes in correspondence with the flesh and red tones (Fig. 1).

Specific questions arose during the conservation treatment, such as knowing the exact number and composition of the overlaying varnishes and overpainting. These questions guided the design of the scientific investigation and methodological approach described herein. After the activities at CCR, the work went on display at the temporary exhibition "Sulle tracce di Raffaello nelle collezioni Sabaude" in the Discovery Section of the MRT in Turin, from October 30th, 2020, to June 2nd, 2021.



Fig. 1 The panel painting *Madonna of the Tent* (inv. 271, Musei Reali Torino, Turin, Italy) before the conservation treatment carried out at CCR in Venaria Reale (Turin, Italy). At right, from top to bottom: details of the brushstrokes of the clouds, the flesh tones in correspondence with the Child's elbow, and the Virgin's blue mantle.

2.2 Scientific investigation and methodological approach

The program of scientific investigation on the *Madonna of the Tent* was first designed by following the general well-established rule based on the conduction of the analyses in subsequent phases. All the noninvasive – imaging and spot – techniques precede the application of micro-invasive methods to minimize the number of samplings, while the outcomes of imaging analyses are used to select the most representative spots of analysis. The methodological approach combining spot and imaging analyses is reported in subsection 2.2.8. It was designed to reach the main goals of the investigation on this multi-layered painting: distinguishing original paints from overpainting and knowing the exact number and chemical composition of the overlayed varnishes. After the data acquisition, all the images, maps, and spots were aligned in a unique file and cross-referenced to exploit the techniques' complementarity. This step was essential to provide hypotheses solid enough on the composition and localization of the artwork materials layer by layer.

2.2.1. Technical photography

Visible diffuse light photography (Vis) was achieved by using two 800W Ianiro Varibeam Halogen lamps (Ianiro, New Taipei City, Taiwan), placed at an angle of approximately 45° to the surface, and with the aid of umbrellas for light diffusion purposes. Photographs were taken using a Nikon D810 Full-Frame DSLR camera (CMOS 7360 4912 pixels).

The ultraviolet-induced visible luminescence (UVL) was acquired via a Nikon D810 full-frame DSLR camera (CMOS 7360 x 4912 pixels) and a Hoya UV-IR cut filter (Hoya, Tokyo, Japan), irradiating the painting with two UV Labino® lamps (365 nm-emission peak).

The infrared reflectography (IRR) was performed using a Nikon D810 full-frame DSLR camera (CMOS 7360 x 4912 pixels), modified to extend the sensor sensitivity range up to 1000 nm, and with a B+W 093 (87c) filter, illuminating the painting using Ianiro Varibeam Halogen 800 W lamps (Ianiro, New Taipei City, Taiwan) with indirect diffused light.

Infrared false color images (IRFC) were obtained in the RGB color space of Adobe Photoshop by using the Vis and IRR images. In particular, the green (G) and red (R) components of the Vis image are transferred into the blue (B) and green (G) channels, while the red (R) component is replaced with the IRR image.

Image processing was carried out by means of Adobe Lightroom and Adobe Photoshop software (Version C6S) and included a color correction conducted by inserting a 24-color ColorChecker Classic reference in the field of view.

2.2.2. Macro X-ray fluorescence (MA-XRF)

MA-XRF analysis was performed using the LANDIS-X mobile X-ray scanner, used in situ at the CCR and developed by the XRAYlab of the Institute of Cultural Heritage Sciences, National Research Council (ISPC-CNR), and by the South National Laboratories, Institute of Nuclear Physics (LNS-INFN), Catania, Italy [21]. LANDIS-X scanner consists of a spectroscopic head equipped with an Rh-anode microfocus tube (50 kV/ 0.6 mA as maximum voltage/current) and two 50-mm^2 silicon drift detectors (SDD), with a 160-eV spectral energy resolution at 5.9 keV working in parallel to record the emitted fluorescence radiation. The primary X-ray beam is transported and focused on the sample by polycapillary optics coupled with the X-ray source. The polycapillary defines a minimum beam size of 50 μm (FWHM) for the Rh-K_α energy at the focus position (i.e. 15 mm from the optic exit): however, MA-XRF analysis in the present study was carried out by positioning the surface out of the polycapillary focus obtaining a spot size of the primary beam of few hundreds of microns. A time list mode (TLIST) implemented in the multi-detector system allows high counting statistics for a time/pixel in the ms range as well as to perform the scanning in continuous mode instead of the conventional step-by-step scan. The spectrometric head is moved during the scanning by using a three-axis XYZ motorized stage presenting a 110 × 70 × 20 cm^3 range. The full area of 110 x 70 cm^2 (XY) scanned in a serpentine manner is covered in less than 2 h at 100 mm/s maximum scanning speed with a pixel size of 1 mm. The Z-axis is dynamically controlled by a laser sensor during scanning to keep the spectrometer head/sample surface

distance. The X-ray scanner developed in real-time technology is fully controlled by a custom-developed control processing unit (CPU). All the acquired X-ray pixel spectra are processed in real-time by applying an accurate fast-fitting procedure and the deconvoluted elemental distribution images are elaborated during the scanning and are available in live mode to be discussed and interpreted by the users [29-30].
The entire *Madonna of the Tent* painting (consisting of c.a. 537 × 802 pixels) was scanned with a speed of 70 mm/s, a dwell time per pixel of 15 ms, and a lateral resolution of 1 mm. The measurement time was 1.8 h and the primary X-ray beam voltage was set at 50 kV, with a current of 600 A.

2.2.3. Hypercolorimetric multispectral imaging (HMI)
HMI is a portable multispectral system developed by the Italian company Profilocolore® consisting of a Nikon D800 modified full-frame camera and two proprietary softwares, one based on AI for calibration and the other for processing the calibrated images [12]. The camera is equipped with two bandpass filters whose spectral transmittances are complementary. The lighting is obtained by two modified flashes controlled by the camera through triggers. The combination of these filters with the Bayer matrix of the camera sensor allows to acquire the spectral range between 300 and 1000 nm with just two photo shoots, subsequently separated into 7 bands by the calibration software (UV; the B, G, R bands of the Vis; IR1 at 750 nm; IR2 at 850 nm and IR3 at 950 nm) providing imaging data with a radiometric accuracy of 95% and colorimetric error $\Delta E<2$. In order to obtain the calibrated images, it is necessary to include acquired scene white radiometric references and a Colorchecker from the Natural Colour System© catalog. The white references must perimeter the scene and include the Colorchecker. The processing software allows for calculating the reflectance values at the seven calibrated wavelengths of each pixel of the image, comparing them with a database of pigments' spectral signatures, elaborating calibrated false color images, and applying chromatic and spectral similarity algorithms and other tools.

2.2.4. Fiber optics reflectance spectroscopy (FORS)
FORS analysis was conducted using an Ocean Optics HR2000+ spectrophotometer, an Ocean Optics HL-2000-FHSA halogen lamp, and a Labsphere Spectralon Wavelength Calibration Standards white reference. The spectral resolution is about 0.5 nm. The system includes two fiber optics, one single and one bifurcated, with a 400-µm diameter, equipped with an Ocean Optics RPH-2 anodized aluminum fiber support, enabling reflection measurements at a 90° or 45° angle to the bearing surface. Spectra were acquired in reflectance mode, within a 360-1000 nm spectral range, with 2x45/0 optical geometry. Spectra were interpreted by comparison with published literature and spectral libraries available at the CCR scientific laboratories [31].

2.2.5. Optical microscopy in visible and ultraviolet light (V is-UV OM) and scanning electron microscopy with energy-dispersive X-ray spectroscopy (SEM/EDS)
A few multi-layered samples were removed from the painting and observed under visible light using an Olympus SZX10 stereomicroscope equipped with an Olympus Color View I digital camera (Olympus Italia S.r.l., Milan, Italy). After being arranged as cross sections, the samples were photographed under visible and ultraviolet light using an Olympus BX51 minero-petrographic microscope equipped with an Olympus DP71 digital camera (Olympus Italia S.r.l., Milan, Italy). In both cases, image acquisition and processing were performed using the analySIS FIVE proprietary software (Version 2005). The cross sections were then analyzed in back-scattered electron mode (BSE) using a Zeiss EVO60 scanning electron microscope equipped with a lanthanum hexaboride (LaB6) cathode (Carl Zeiss Microscopy GmbH, Jena, Germany) and a silicon drift detector (SDD), coupled with a 40 mm^2 Oxford Ultim Max EDS microprobe (Oxford Instruments NanoAnalysis, Gometz la Ville, France) for semi-quantitative elemental analysis. They were coated with a nanometric layer of carbon and analyzed in high vacuum mode, using an accelerating voltage of 20 kV and a pressure of 10^{-5} Pa.

2.2.6. Fourier-transform infrared (FTIR) spectroscopy

FTIR analysis on selective samples was performed with a Bruker Vertex 70 FTIR spectrometer coupled with a Bruker Hyperion 3000 infrared microscope and equipped with a mercury cadmium telluride (MCT) detector. Scrapings were analyzed as a bulk in transmission mode through a 15x objective, upon compression in a diamond cell. Data were collected in the 4000-650 cm^{-1} spectral range, at a spectral resolution of 4 cm^{-1}, as the sum of 32 scans. Spectra were interpreted by comparison with published literature and spectral libraries available at the CCR scientific laboratories.

2.2.7 Py-GC/MS

The selective samples of varnishes removed from the painting were analyzed by pyrolysis-GC/MS using a micro-furnace EGA/PY-3030D pyrolyzer (Frontier Lab, Japan) interfaced with a 6890N Network GC System gas chromatograph (Agilent Technologies, USA) equipped with HP-5 cross-linked 5% Ph Me Silicone capillary column (30 m, 0.25 mm i.d., 0.25 μm film thickness) and a 5973 Network Mass Selective Detector mass spectrometer (Agilent Technologies, USA).

Samples were derivatized with the Thermally Assisted Hydrolysis and Methylation method (THM) using tetramethylammonium hydroxide (TMAH) in an aqueous solution at a concentration of 25% by weight (Sigma-Aldrich, Italy).

Pyrolysis was carried out at 500°C for 12 s. The interface temperature of the pyrolyzer was 300 °C and the temperature of the GC injector was kept at 280 °C. For the gas chromatographic separation, the following temperature program was used: 2-minute isotherm at 50 °C, ramp of 10 °C/min up to 300 °C, isotherm at 300 °C for 15 minutes. The mass spectra, obtained by electron impaction at 70 eV, were recorded in the range 40-650 m/z. The carrier gas used is helium, with a flow rate of 1.0 ml/min. All instruments were controlled by Enhanced Chem Station (ver. 9.00.00.38) software. The mass spectra assignment was done with the Wiley 138 and NIST2008 libraries and by comparison with literature data.

2.2.8 Methodological approach

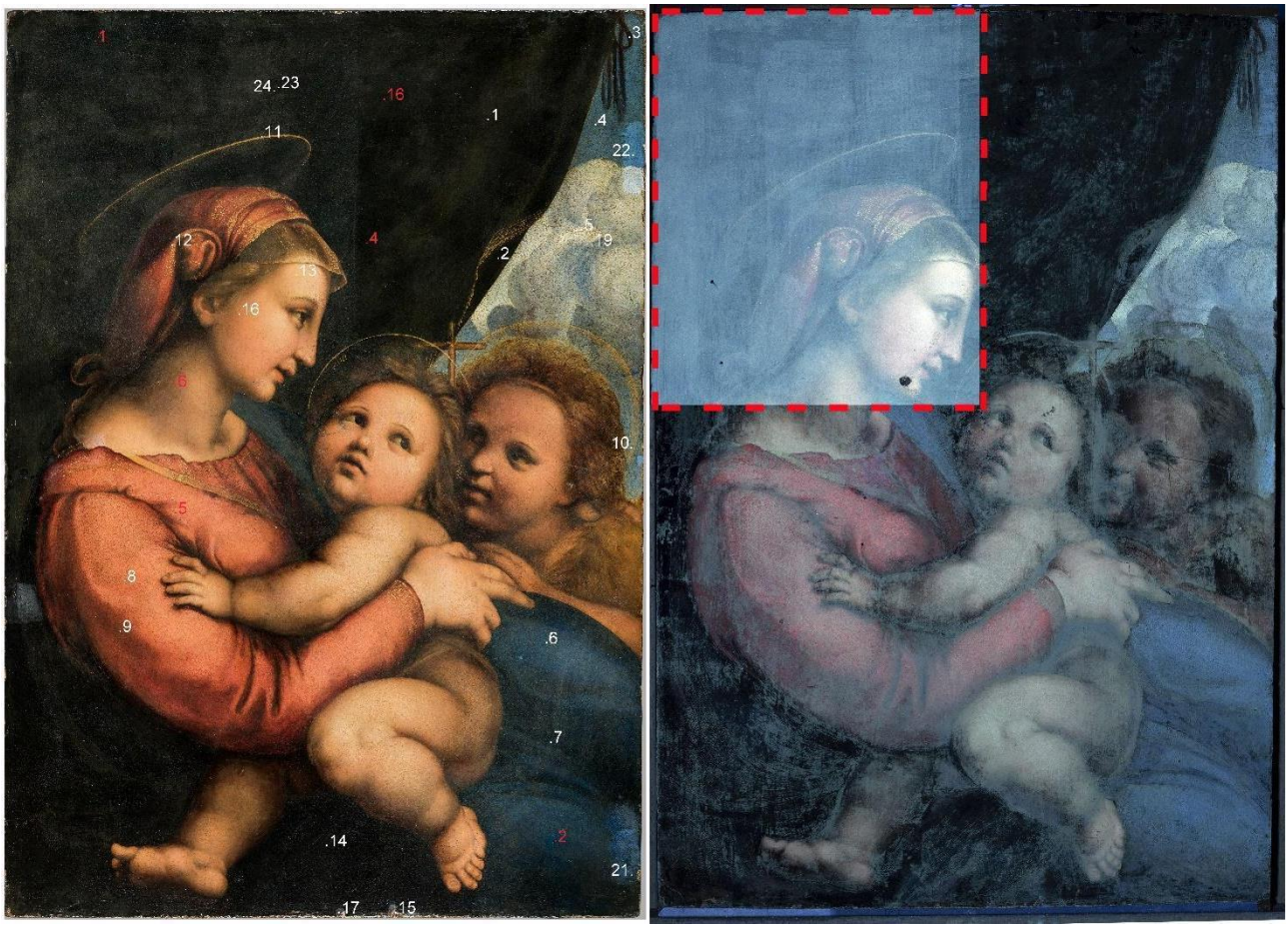
Technical photography – that is Vis, UVL, IRR, IRFC – was the first step of scientific investigation, since it provides an overview of the different painting materials based on their different reflectance or luminescence concerning the irradiation wavelengths.

MA-XRF was subsequently applied to characterize and distinguish original paints and overpainting through the chemical mapping of the painted surface. HMI was used to collect general information on the painting materials and make the first hypotheses about composition. Some postprocessing tools, such as chromatic similarity, were applied to HMI data to facilitate the following steps of the analytical process and the selection of the spots of analysis. FORS analyses were thus performed on selected spots (Fig. 2a) to recognize pigments and lakes of the outermost layers based on their reflectance and absorption features. MA-XRF, HMI, and FORS data were cross-referenced for a complete palette characterization.

Among technical photography techniques, UVL was acquired both before and during the conservation treatment: images acquired during the cleaning tests for removing the not original varnishes were used for cross-referencing the information about the varnishes' luminescence with their chemical characterization coming from micro-invasive analyses (Fig. 2b).

Regarding micro-invasive analyses, some multi-layered samples were removed from the painting and analyzed to understand the stratigraphy and possible differences within the work, which could have suggested previous localized treatments. These samples come from the main areas of the painting: the green curtain, the Virgin's red dress, her blue mantle, and her flesh tone (Fig. 2a). The cross sections were compared with each other to verify the exact number of paint and varnish layers. The latter ones were observed and distinguished under UV light. Therefore, a sampling method based on the UV images of the cross sections was designed to remove one by one the varnish layers and allow subsequent micro-invasive analyses. Scrapings of both varnishes and paint layers were analyzed via FTIR (Fig. 2a, red spots) to provide preliminary information on the classes of organic and inorganic compounds, as functional to the chromatographic analyses. The green area of the curtain was

chosen for the Py-GC/MS analyses (Fig. 2a, red spot n° 16). Both for FTIR and Py-GC/MS, samples were taken with a scalpel, delicately scratching the surface of the painting to remove the different varnishes observed in the cross sections. During the sampling, the transition from one varnish layer to the other was checked by observing the change in the UVL of the surface. It was thus possible to take four micro-samples representative of four layers of varnish.



a *b*

Fig. 2 The work during the conservation treatment: *a)* Vis-D image during the first cleaning tests for removing the not original varnish, with sampling sites (in red) and spots of noninvasive FORS analysis (in white); *b)* UVL during the progressive removal of non-original varnishes, with a red box in the upper left documenting the initial state.

4. Results and Discussion

3.1 The paint layers: materials and techniques

The cross-reference of data collected from MA-XRF, HMI, FORS, FTIR, UV-Vis OM, and SEM/EDS allowed for shedding light on the art materials and technique of the *Madonna of the Tent* painting.

Especially, MA-XRF provided the first crucial information, namely the distribution of the chemical elements over the surface of the work. Figure 3 shows the correlation maps of the most significant chemical elements. As discussed in [1], calcium, lead, and iron signals are omnipresent and distributed fairly uniformly, suggesting they come (also) from the preparatory layers. Other chemical elements – such as copper, manganese, and cobalt – are localized on delimited areas of paint, suggesting their signals come more likely from the pigments of the paint layers. For example, cobalt, likely coming from smalt, was detected in correspondence with the Virgin's eye, details of the blue robe, and shadows of the clouds. All other observations followed from these chemical maps. For example, the green curtain and Virgin's blue mantle answered similarly in MA-XRF, copper-based

pigments: the information from HMI and the spectral reflectance factor collected via FORS led to an improved pigment characterization; finally, the analysis of the cross-sections added further decisive data.
This process allowed for identifying the use of lead white, gold, azurite, smalt, lapis lazuli, copper-based green, copper resinate, cinnabar, red and yellow ochres, lead-tin yellow, and madder lake, confirming the compatibility with 16th-century manufacturing. Proceeding by color fields, the results of the investigations on flesh tones, the red of the Virgin's robe, the blue of her mantle, and the green of the curtain are reported below.

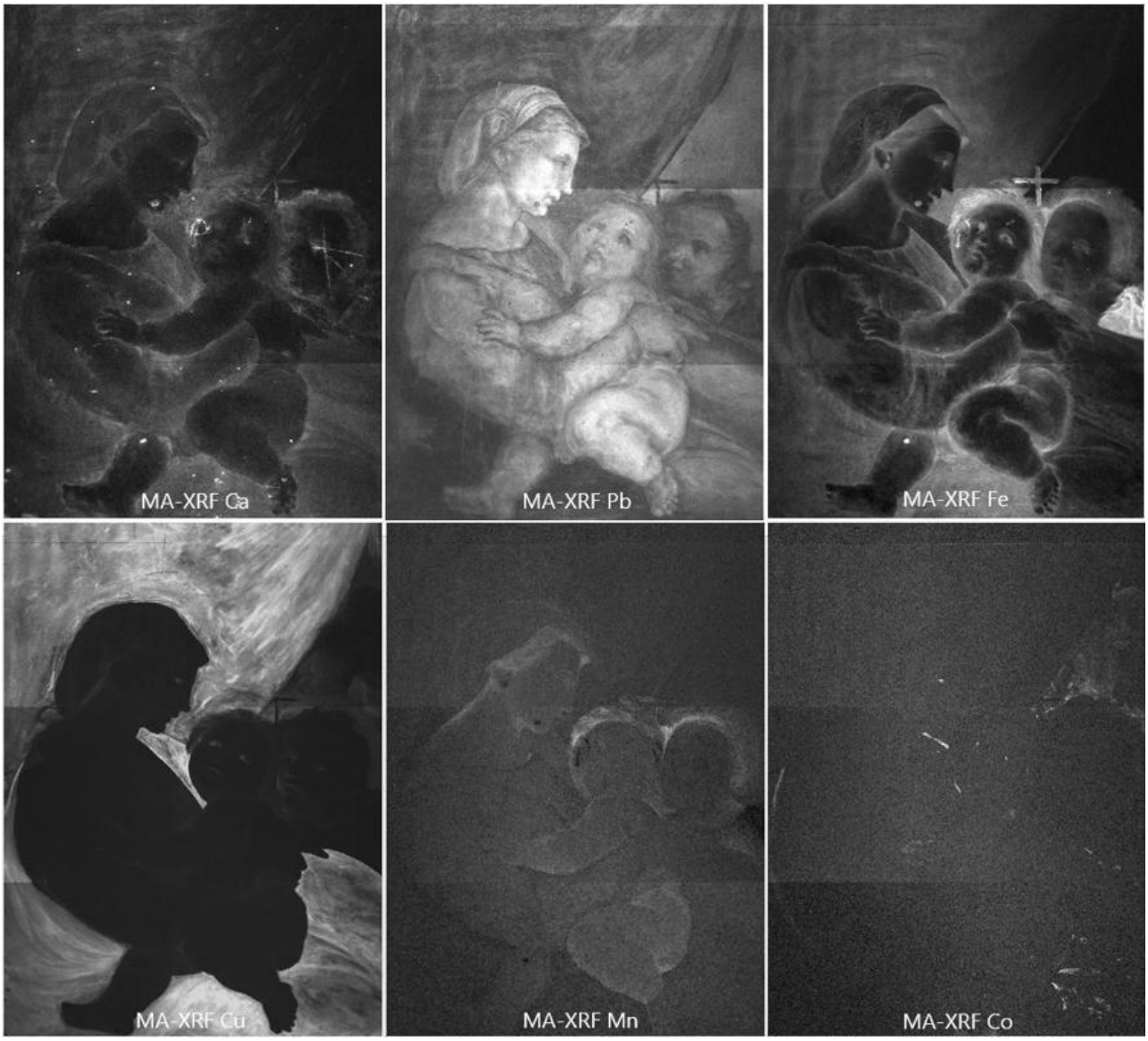


Fig. 3 MA-XRF maps of calcium (Ca), lead (Pb), iron (Fe), copper (Cu), manganese (Mn), and cobalt (Co).

3.1.1 The Virgin's red robe and flesh tones

In correspondence with the Virgin's red robe, the MA-XRF maps showed the presence of a lead-based pigment, likely lead white, with few amounts of iron. This iron signal, likely attributable to ochres and majorly distributed in the shadows, is so low that it cannot be responsible for the intense red of the robe (see Fig. 3). Moreover, the UVL of the robe after the removal of the outermost layers of varnish (see Fig. 2b), suggested the presence of some organic or lake pigments [32-35]. In this case, the reflectance spectrum was decisive for identifying which component contributes the most to giving the robe that color. The chromatic similarity map obtained through HMI processing software showed the distribution of the red in the Virgin's robe (Fig. 4a: the

white pixels have high similarity among them, black pixels have no similarity). However, no match was found in the database supplied by Profilocolore, that could be compatible with the MA-XRF results. FORS analysis, in the same point selected for chromatic similarity application, allowed for identifying the typical spectral behavior of a madder lake (Fig. 5a, gray curve) [36-38], which is responsible for that intense UVL. In the multi-layered sample of the red robe, the madder lake layer is well visible thanks to the intense, pink UV-induced luminescence: it is made of an outer glazing of madder lake alone (Fig. 6a at left, layer 4) and an inner layer where madder is mixed with lead white and minor amounts of red ochre (layer 3). Interestingly, the sample also shows the presence of a yellow *imprimitura* made of lead white and yellow ochres, with rare grains of red ochres (layer 2). The presence of several grains of bone's black at the bottom of this layer can come from the underdrawing [1]. The outermost layers of the sample, mainly organic, will be discussed later.

As far as flesh tones are concerned, the MA-XRF maps indicate the presence of white lead as the majority element (see Fig. 3). Chromatic similarity tool of HMI processing software was applied to the flesh tone of the Virgin face, in correspondence with the darker zone. The algorithm is able to well-differentiate this zone from the lighter one of the cheek, of the forehead and of the other light areas of the flesh tones (Fig. 4b). Here the FORS spectrum, acquired in a more saturated red area, indicates the presence of cinnabar and madder lake (Fig. 5a, black curve). Analysis of a multi-layered sample coming from the Virgin's neck confirms the chemical composition of the mixture: the paint contains lead white, with minor amounts of ocher and cinnabar, and rare grains of madder lake; the sample also shows the presence of the yellow *imprimitura* above the gypsum-based ground (Fig. 6a, right).

Overall, no overpainting was observed in the Virgin's red robe and flesh tones.



a *b*

Fig. 4 Result of the chromatic similarity tool applied to the painting in the points highlighted by the red dots: *a)* red robe of the Virgin; *b)* dark flesh tone of the Virgin's face.

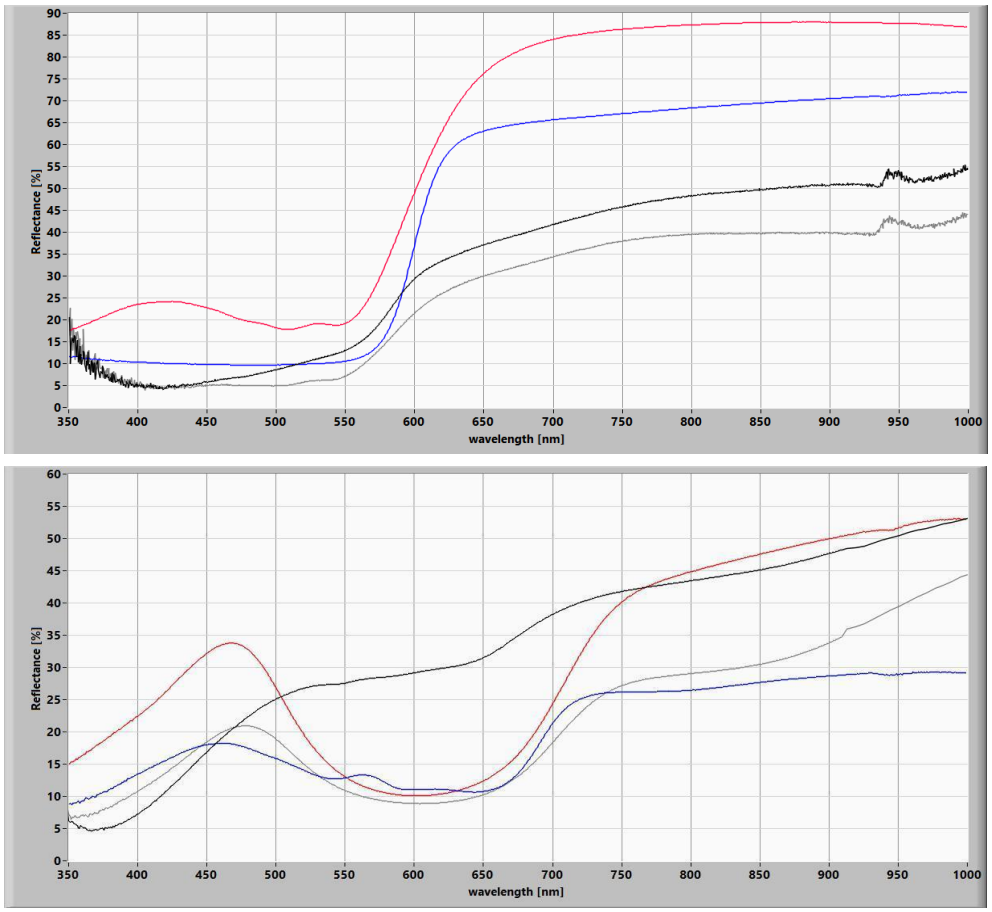


Fig. 5 FORS spectra of: *a)* the Virgin's red robe (gray curve) and her neck (black curve), respectively identified by the white spots n° 8 and n° 16 in Fig. 2a, compared to the database reference spectra of mock-ups made with madder lake (red curve) and cinnabar (blue curve); *b)* the blue sky (grey curve) and light blue cloud (black curve), white spots n° 22 and n° 5 in Fig. 2a, compared to reference spectra of lapis lazuli (red curve) and smalt (blue curve).

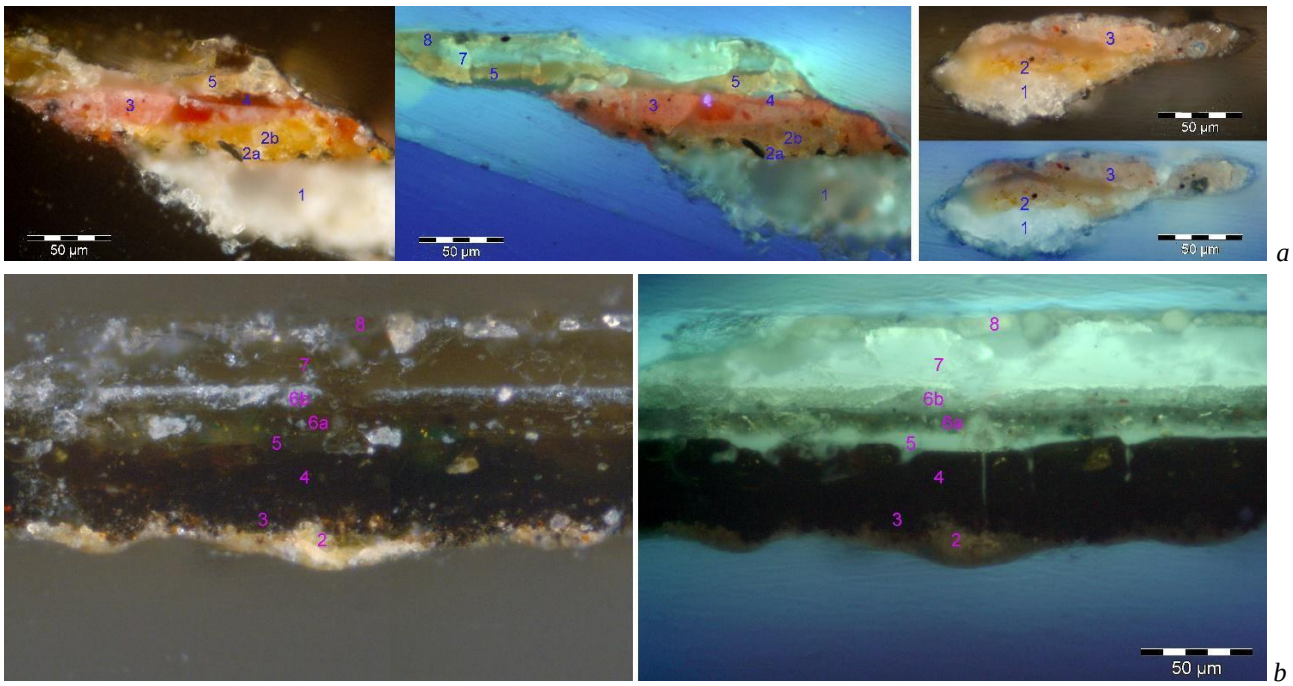


Fig. 6 Vis-UV OM images of: *a)* the multi-layered samples from the Virgin's red robe (at left) and her neck (at right), respectively identified by the red spots n° 5 and n° 6 in Fig. 2a; *b)* the multi-layered sample from the green curtain (red spot n° 4 in Fig. 2a).

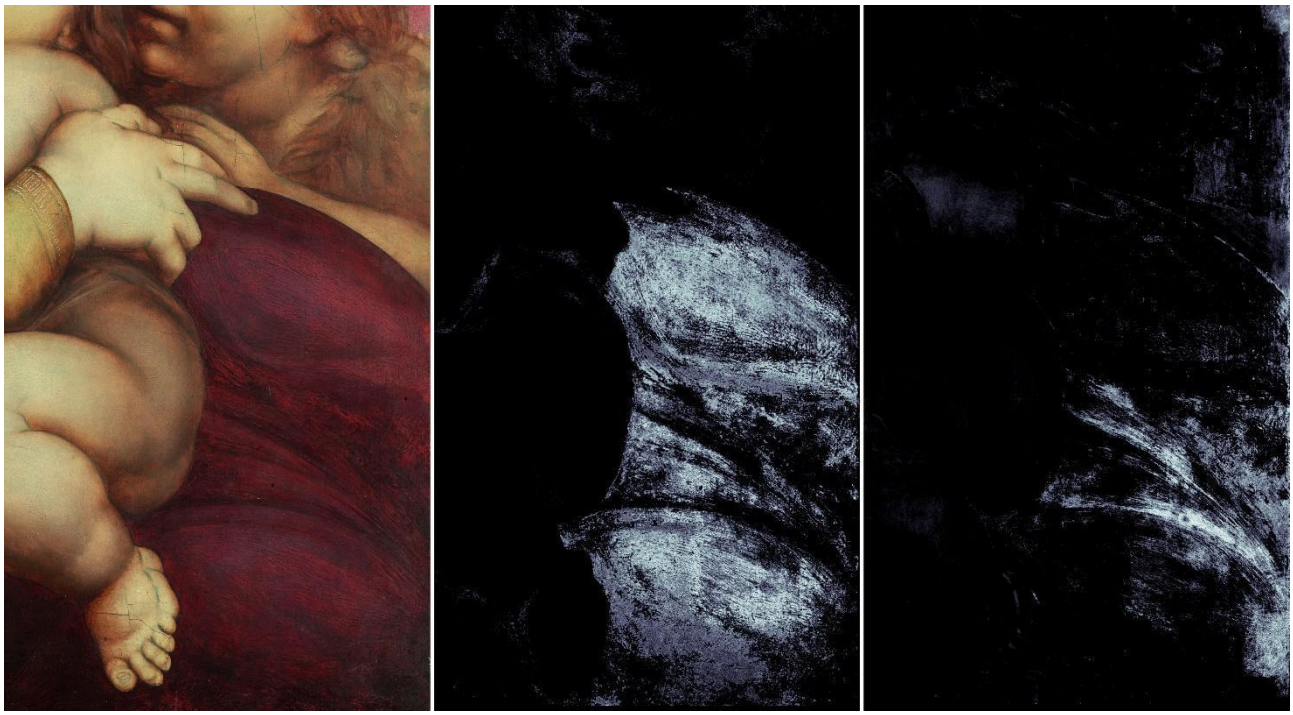
3.1.2 The blue of the Virgin's mantle and sky

The MA-XRF maps on the Virgin's blue mantle indicated the presence of copper as a major chemical element, suggesting the presence of azurite, with only some small cobalt-based details (see Fig. 3).

In this case, the IRFC image was decisive since it showed that most brushstrokes over the blue surface have a red false color, which can be associated with the presence of lapis lazuli rather than with a copper-based blue pigment such as azurite (Fig. 7). This pigment turning red in IRFC seems to cover a further underlying paint layer, which has instead a dark false color attributable to azurite, thus explaining the intense XRF signal of copper.

Thanks to the application of the HMI, the diffuse brushstrokes on the surface of the blue mantle were mapped and identified as possible lapis lazuli, while the darker areas are compatible with azurite. As shown in Figure 7, the two HMI maps relating to the distribution of the hypothesized lapis lazuli and azurite on the surface are almost complementary, while it is not possible to distinguish the smalt-based detail indicated by MA-XRF.

The spot analyses via FORS allowed for documenting the spectral behavior of the lapis lazuli on several spots of the blue mantle. A multi-layered sample (see Fig. 2a, red spot n° 2) confirmed the layering of the two main pigments – lapis lazuli above and azurite below. Moreover, FTIR analysis of a scraping from the superficial blue paint confirmed the presence of silicates – referring to lapis lazuli – and detected the use of a drying oil as a binder (Fig. 8a).



a *b* *c*

Fig. 7 Detail of the Virgin's blue mantle: *a)* IRFC; *b)* and *c)* are HMI spectral similarity maps indicating respectively the localization of lapis lazuli and azurite.

As for the area of the sky, the intense blue was identified as lapis lazuli via FORS (Fig. 5b , grey and red curves); the small copper-based details localized via MA-XRF on the clouds (see Fig. 3) were also analyzed by FORS and the reflectance spectra confirmed the presence of smalt (Fig. 5b , black and blue curves).

Based on these results, all the pigments identified in the blue of the Virgin's mantle and sky are compatible with those in use at the time the painting was made.

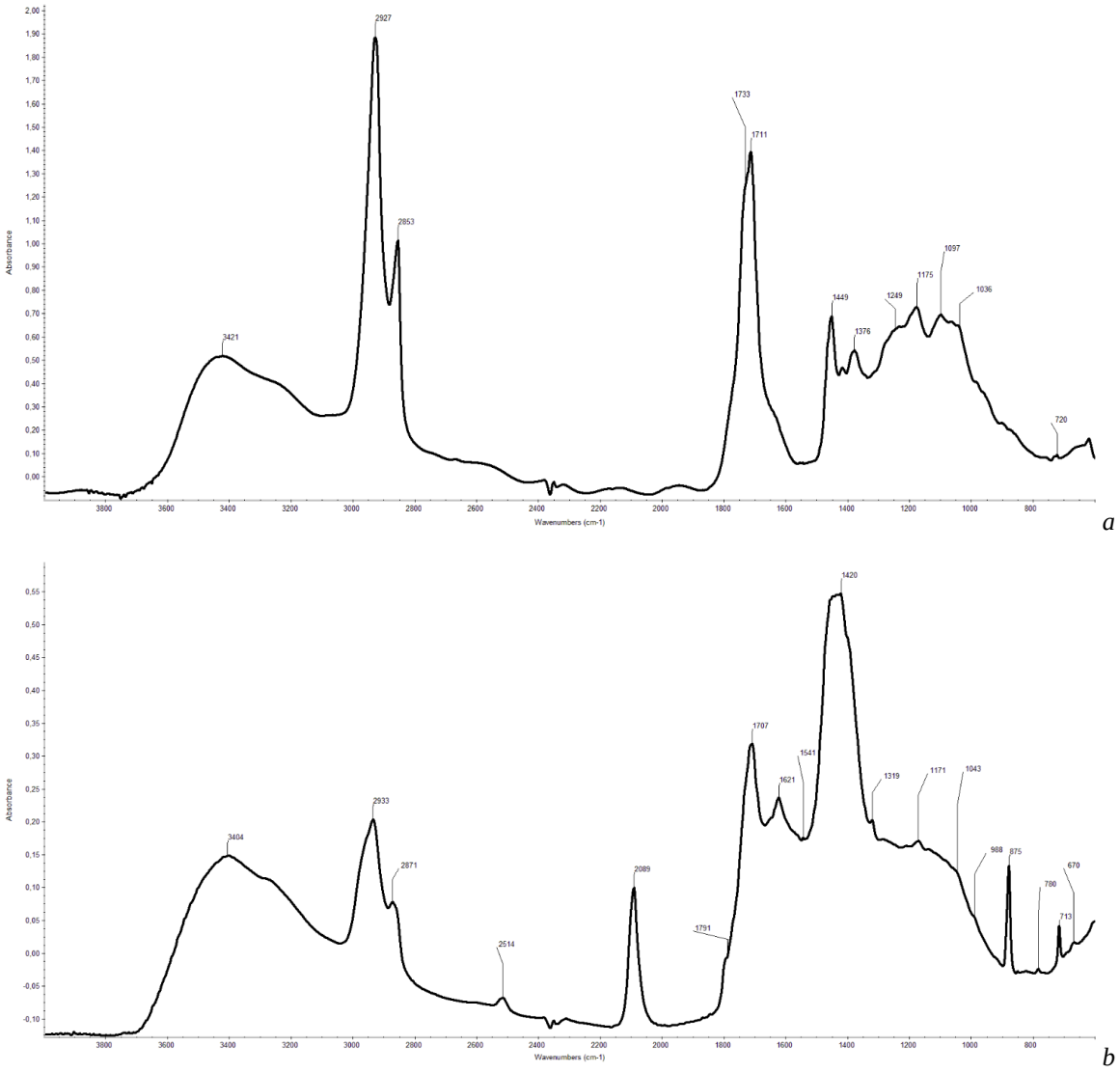


Fig. 8 *a)* FTIR spectrum of a scraping selectively removed from the original blue layer: spectral features of an aged drying oil were detected: 2927, 2853, 1733, 1711, 1449, 1376, 1249, 1175 cm^{-1}. Signals at 1097 and 1036 cm^{-1} were assigned to silicates, attributable to lapis lazuli. *b)* FTIR spectrum of a scraping selectively removed from layers 6a and 6b in the 400-4000 cm-1 range: diagnostic band for Prussian Blue at 2089 cm-1 was detected; 2514, 1791, 1420, 875, 713 cm-1 were assigned to calcite; 1171, 1043 cm-1 to silicates; 2933, 2871, 1707 cm-1 to natural resin, and 1621, 1319 cm-1 to oxalates. 1541 cm-1 signal was attributed to zinc stearate.

3.1.3 The green curtain

Before the conservation treatment, the color of the curtain against the background of the painting appeared dark brown, although iconography would have suggested it to be green. Based on the outcomes of the non-invasive analyses, we first hypothesized the presence of copper resinate, whose sensitivity to oxidation and degradation phenomena is well attested [39-40]. The MA-XRF maps indicated the presence of copper as the main chemical element, and FORS spectra suggested the presence of copper green or copper resinate, having similar reflectance spectra [41].

Here the analysis of a multi-layered sample was decisive for understanding both the chemical composition and the history of previous conservation treatments that the work underwent over the years. Vis-UV OM images of the cross section show the presence of a copper resinate layer with rare grains of mineral copper-based green

(Fig. 6b , layer 4) – detected by SEM/EDS – over a dark layer of carbon black with small amounts of ochres and lead white (layer 3). Both these layers are attributable to the original art technique, and the presence of copper resinate would explain the bad preservation of the curtain. The presence of organic layers on the top of the sample will be discussed later. However, it is worth noting that the green curtain is the only area where the cross section undoubtedly indicates the presence of overpainting. In fact, EDS analysis of layers 6a and 6b – so named because they look like two coats of the same paint – actually allowed for detecting the presence of rare grains containing chrome, lead, iron, and copper diffused within a mostly organic matrix. FTIR analysis of a scraping selectively removed from those layers indicated the presence of Prussian blue and natural resin (Fig. 8b). That led to interpreting those layers as resin-based, slightly colored overpainting containing Prussian blue and chrome yellow, therefore a green translucent, undoubtedly modern overpainting. The introduction of lead chromate, or chrome yellow, as a pigment is attested between 1804 and 1809 [42]. In the following decades of the nineteenth century, the terms “chromium green” and “cinnabar green” indicate a composite pigment where Prussian blue is precipitated on chromium yellow. This mixture makes a beautiful green but degrades over time, resulting in unsuitable for the fine arts [42].

3.2 Varnishes

The glossy appearance and intense UVL of the work before the conservation treatment already indicated the presence of thick layers of varnish over the surface. The UV OM images of the cross sections allowed for counting three layers of varnish on the painted surface with a similar stratigraphy in all the samples except for the green curtain: here, the green overpainting described above is present between the innermost layer of varnish (see Fig. 6b , layer 5) and the following one (layer 7).

FTIR analysis on scrapings selectively removed by scalpel gave preliminary data about the chemical composition of these varnishes, and Py/GC-MS was decisive for the identification.

Although the thickness of the layers did not allow a truly selective sampling of the varnishes, Py-GC/MS analyses pointed out differences in the composition of the various layers, thus allowing the stratigraphy to be linked to the conservation history of the painting. Table 1 lists all compounds identified in the Py-GC/MS curves shown in Figure 12.

Table 1 Lists of compounds identified by Py-GC/MS. Due to methylation with TMAH acidic groups are detected as methyl esters and hydroxy groups as alkoxy derivatives.

Peak No.	**Retention time (min)**	**Assignment**	**Layers of varnishes and overpainting numbered as in Fig. 6b**			
			n. 5	**n. 6**	**n. 7**	**n. 8**
1	5.2	1,2,3-trimethoxypropane	X	X	X	X
2	13.4	Octanedioic acid dimethyl ester	X	X	X	
3	14.7	Nonanedioic acid dimethyl ester	X	X	X	X
4	16.7	Tetradecanoic acid methyl ester	X	X	X	X
5	17.7	Pentadecanoic acid methyl ester	X	X		X
6	18.8	Hexadecanoic acid methyl ester	X	X	X	X
7	20,4	9-octadecenoic acid methyl ester	X			X
8	20.7	Octadecanoic acid methyl ester	X	X	X	X

9	22.7	Unidentified compound (m/z 69, 137, 157, 169, 185, 201, 327)	X			
10	22.7	Dehydroabietic acid methyl ester	X	X		
11	23.5	7-methoxydehydroabietic acid methyl ester	X	X		
12	23.6	7-methoxytetradehydroabietic acid methyl ester	X	X	X	
13	24.1	15-hydroxy-7-oxodehydroabietic acid methyl ester	X	X		
14	24.8	7,15-dimethoxytetradehydroabietic acid methyl ester	X	X	X	
15	31.1	3,4-seco-olean-18-en-3,28-dioic acid methyl ester	X	X		
16	32.1	Moronic acid methyl ester (3-oxo-olean-18-en-28-oic acid methyl ester)	X	X		
17	32.1	Unidentified compound (m/z 151, 189, 219, 482)	X	X		
18	32.4	3-oxo-18αH-olean-12-en-28-oic acid methyl ester	X	X		
19	32.7	Unidentified compound (m/z 145, 271, 435, 451, 510)	X	X		
20	33.0	Unidentified compound (m/z 145, 165, 189, 233, 453, 496)	X	X		
21	33.3	Unidentified compound (m/z 112, 189, 428, 465, 524)	X	X		
22	33.6	Unidentified compound (m/z 189, 421, 496)	X	X		
23	33.6	Unidentified compound (m/z 465, 511, 524)	X	X		
24	14.3	Dodecanoic acid methyl ester		X	X	X
25	15.0	Longicamphenylone		X	X	
26	15.2	3,4-dimethoxybenzoic acid methyl ester		X		
27	19.7	Unidentified compound (m/z 102, 146, 256)		X	X	X
28	20.2	Unidentified compound (m/z 88, 102, 132, 242, 256)		X	X	X
29	20.5	Unidentified compound (m/z 102, 116, 169, 256, 270)		X		
30	21.5	Unidentified compound (m/z 102, 146, 284)		X	X	X
31	23.2	Unidentified compound (m/z 102, 146, 312)		X	X	X
32	3.3	3-methylenecyclohexene			X	
33	5.1	Cyclohexanone			X	
34	5.6	Hexanoic acid methyl ester			X	
35	6.0	2-methylcyclohexanone			X	
36	6.5	2-methylenecyclohexanone			X	
37	8.9	Octanoic acid methyl ester			X	
38	9.1	Pentanedioic acid dimethyl ester			X	
39	9.7	2,3-dimethoxytoluene			X	
40	10.3	Nonanoic acid methyl ester			X	

41	10.7	Hexanedioic acid dimethyl ester			X	
42	11.5	Unidentified compound (m/z 55, 57, 69, 71, 83, 85, 97, 111, 125, 153, 154)			X	X
43	11.8	Unidentified compound (m/z 55, 57, 69, 71, 83, 85, 97, 111, 125, 154)			X	X
44	12.1	Heptanedioic acid dimethyl ester			X	
45	12.9	Unidentified compound (m/z 55, 69, 83, 96, 114, 128, 139, 141, 151, 154 182, 183)			X	
46	13.0	Decahydro-4,8,8-trimethyl-9-methylene-1,4-methanoazulene (longifolene)			X	
47	16.8	Methylcyclohexanone dimer			X	
48	16.9	Methylcyclohexanone dimer			X	
49	17.0	Methylcyclohexanone dimer			X	X
50	17.1	Methylcyclohexanone dimer			X	X
51	21.0	Methylcyclohexanone trimer			X	
52	21.3	Methylcyclohexanone trimer			X	
53	21.7	Methylcyclohexanone trimer			X	
54	22.2	Methylcyclohexanone trimer			X	
55	27.0	Methylcyclohexanone tetramer			X	
56	27.6	Methylcyclohexanone tetramer			X	
57	18.5	9-hexadecenoic acid methyl ester				X
58	20.4	14-methoxyhexadecanoic acid methyl ester				X
59	20.5	15-methoxyhexadecanoic acid methyl ester				X
60	22.4	Eicosanoic acid methyl ester				X
61	24.1	Docosanoic acid methyl ester				X
62	25.6	Tetracosanoic acid methyl ester				X
63	26.3	Squalene				X
64	27.0	Hexacosanoic acid methyl ester				X
65	27.7	1-methoxyoctacosane				X
66	28.5	Octacosanoic acid methyl ester				X
67	29.4	1-methoxytriacontane				X
68	31.7	1-methoxydotriacontane				X

Starting from the inside and moving toward the surface, the oldest varnish (layer 5, see Tab. 1 and Fig. 6b) is oleoresinous, based on siccative oil, combined with di- and triterpenic resins (Fig. 9 a). The main marker compounds of siccative oils are the methyl esters of suberic acid (octanedioic acid, peak n. 2 of Tab. 1), azelaic

acid (nonanedioic acid, peak n. 3), myristic acid (tetradecanoic acid, peak n. 4), palmitic acid (P, peak n. 6), stearic acid (S, peak n. 8) and traces of oleic acid (peak n.7). The A/P ratio, based on peak areas, is 0.7 and confirms the siccative nature of the oil. The P/S ratio is 2.3, a value close to the upper limit found in the literature for linseed oil (i.e. 2.5 [43, 44]) and in a range more characteristic of walnut oil [43, 45, 46]. The diterpenoids identified in the pyrograms are markers of Pinaceae resins like colophony. More specifically the three relatively intense peaks eluted between 22 and 25 minutes of retention time are assigned to dehydroabietic acid (peak n. 10), 7-hydroxydehydroabietic acid (peak n. 11), 7-hydroxytetradehydroabietic acid (peak n. 12), 15-hydroxy-7-oxodehydroabietic acid (peak n. 13) and 7,15-dihydroxytetradehydroabietic acid (peak n. 14) [47]. At higher retention time, between 30 and 35 minutes, several peaks point to the presence of less volatile components. Although the interpretation of mass spectra corresponding to these peaks was not easy due to coelution of more species, the methyl esters of moronic acid (3-oxo-olean-18-en-28-oic acid, peak n. 16) and 3-oxo-18αH-olean-12-en-28-oic acid (peak n. 18), that are characteristic triterpenoids contained in mastic were identified [48]. Another chromatographic peak was tentatively assigned to 3,4-seco-olean-18-en-3,28-dioic acid, which may result from the oxidation of moronic acid by breaking the bond near the carbonyl in position 3 according to the Norrish reaction.

Other peaks remain unknown. Although they can all be referred to compounds with a molecular weight similar to that of oxidized triterpenes, it has not been possible to identify them with certainty, nor to establish whether they are products of oxidation of the mastic resin or additional components of the varnish.

The oldest varnish is followed by a layer of similar composition but it is clearly recognizable in the stratigraphy (layer 6) because of the presence of some compounds that lower the UV fluorescence. As already described in section 3.1.3, this layer was detected only on the area of the green curtain and is actually a modern overpainting containing rare particles of Prussian blue and chrome yellow dispersed in an oleoresinous matrix. The relative intensities of the fatty acids, diterpenic markers, and triterpenic markers (Fig. 9 b) of the overpainting are the same as the varnish below (Fig. 9 a) and also the A/P and P/S values, which are 0.8 and 2.3 respectively, demonstrate that the oleoresinous components of these first two layers have a similar composition.

The varnish above (layer 7) is still oil-based but with low colophony content and no mastic. Compounds assigned to monomers, dimers, trimers, and tetramers of a ketone resin have been identified (Fig. 9c) [49, 50]. Even if the peaks of ketone resin markers have relatively high intensity, these are probably contaminations of the most superficial varnish layer (layer 8), in which, in addition to traces of ketone resin and oil, beeswax was detected as the main component (Fig. 9 d). In fact, long-chain fatty acids (peaks n. 60, 61, 62, 64, 66) and long-chain alcohols (peaks n. 65, 67, 68) have been identified, as well as characteristic hydroxyacidss of beeswax such as 14-hydroxyhexadecanoic acid and 15-hydroxyhexadecanoic acid (peak n. 59) [51, 52]. The P/S and A/P ratios calculated for this layer of the painting, equal to 3.4 and 0.2 respectively, confirm that the fatty acid profile results from a combination of different components, with a predominance of beeswax and a lower presence of drying oil. Overall, the Py-GC/MS analyses indicate that the outermost layer of varnish is a waxy ketone varnish which itself exhibits a layering of its two components, with the ketone resin localized at the interface with the underlying varnish layer and the waxy component stratified on the surface exposed to the air.

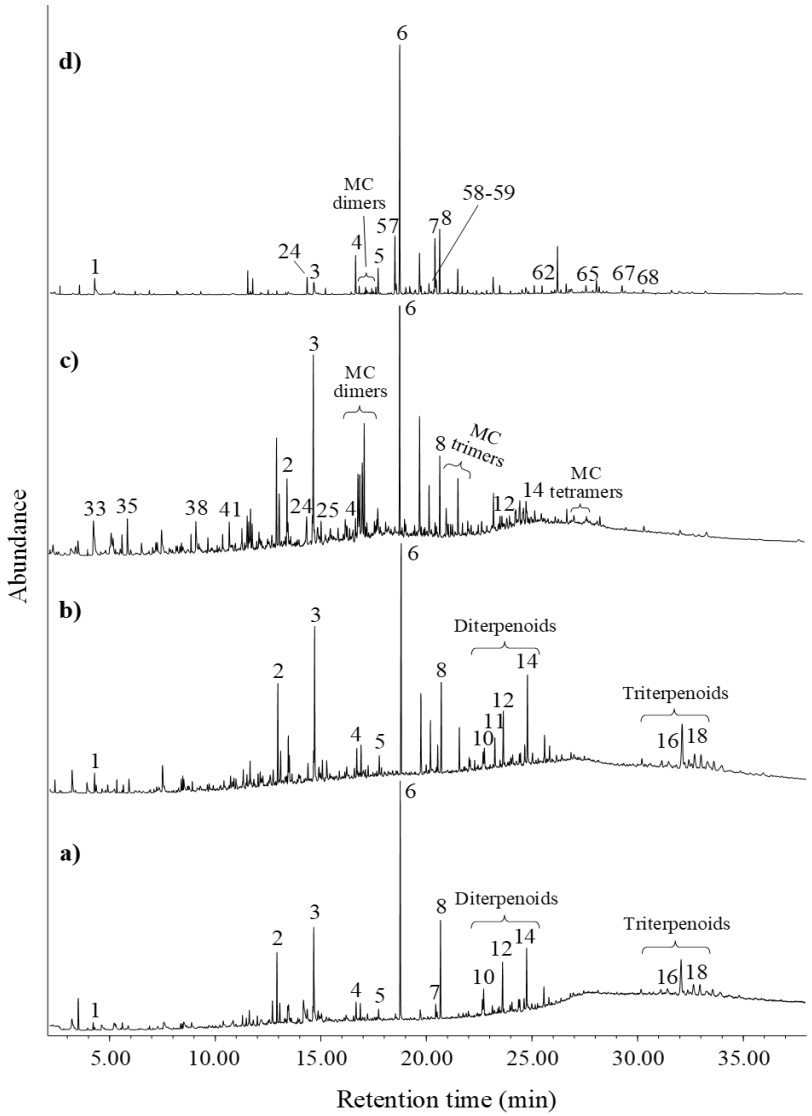


Fig. 9 Py-GC/MS analysis of the three layers of varnish and the layer of overpainting: a) the oldest varnish, b) the overpainting, c) the intermediate varnish, d) the most recent varnish. Peak numbers refer to Table 1. MC: methylcyclohexanone.

5. Conclusions

The scientific analyses and methodological approach applied to the *Madonna of the Tent* of Turin allowed for supporting the conservation treatment carried out in the years 2018-2020 at CCR. The two main aims of the scientific investigation were knowing the exact number and composition of the overlaying varnishes and detecting possible overpainting, necessarily starting from the study of the original material and technique.

This case study demonstrates that combining MA-XRF, HMI, and FORS is effective for studying the paint layers, preliminary to any detection of overpainting. MA-XRF analysis provides crucial information on the chemical composition and distribution of the pigments. The spectral or chromatic similarity maps obtainable through HMI processing software can show the distribution of the colors over the painting, allowing for making hypotheses about the pigments. Vis-NIR FORS can be decisive for identifying many materials, such as lapis lazuli, azurite, smalt, and madder lake. Therefore, integrating these complementary techniques can provide data solid enough about the material of the work in a non-invasive way.

On the other hand, we demonstrate that removing and analyzing multi-layer samples might still be necessary

to add decisive data on pigments and varnish layering, especially for supporting conservation treatment.
In this work, observing and comparing the cross sections under UV light was fundamental to distinguish the different varnishes and overpainting applied over time on the surface of the painting. These layers showed in fact slightly different luminescence and this was crucial during the cleaning tests for removing the not original varnishes, and during the conservation treatment itself. Moreover, the comparison among the cross sections allowed for an immediate understanding of the presence of overpainting in the green curtain: while the other samples showed the same layering of varnishes, an extra layer – between the first and the second varnish – was detected in the green curtain.
The difference in UVL was likewise exploited for selectively removing the scrapings for the micro-invasive chemical analyses.
As for the varnishes, Py-GC/MS of these scrapings made it possible to reveal their chemical composition. The oldest varnish is oleoresinous and consists of siccative oil, diterpene resin, and mastic. Above is another oleoresinous varnish based on siccative oil and diterpene resin, but without mastic. Finally, the most recent varnish is based on ketone resin and beeswax. Considering the variety of organic components present in each varnish and the reduced thickness of the layers, from about 10 to 25 μm, the applied methodology proved to be very effective.
As for overpainting in the green curtain, combining the information from SEM/EDS, Py-GC/MS, and FTIR led to the identification of a mixture of oleoresin and modern pigments, i. e. yellow chrome and Prussian blue. Originally the curtain was supposed to have an intense color, and this color mixture was probably intended to remedy a chromatic alteration of the green. Therefore, the applied methodology proved to be effective for studying overpainting too.
Such information was of great importance for shedding light on the history of the work and its past conservation treatments.

References

[1] T. Cavaleri, C. Pelosi, M. Ricci, S. Laureti, F. P. Romano, C. Caliri, B. Ventura, S. De Blasi, M. Gargano, *IR Reflectography, Pulse-Compression Thermography, MA-XRF, and Radiography: A Full-Thickness Study of a 16th-Century Panel Painting Copy of Raphael*, Journal of Imaging 2022, 8, 150. https://doi.org/10.3390/jimaging8060150, 2022
[2] T. Cavaleri, C. Pelosi, R. Giustetto, A. Andreotti, I. Bonaduce, G. Calabrò, C. Caliri, C. Colantonio, P. Manchinu, S. Legnaioli, A. Piccirillo, F. P. Romano, B. Ventura, G. Ferraris di Celle, M. Gargano, *The northern-Italy Renaissance in a panel by Defendente Ferrari: a complete study with a multi-analytical investigation*, Journal of Archaeological Science: Reports, Volume 46, 2022, 103669, ISSN 2352-409X, https://doi.org/10.1016/j.jasrep.2022.103669 2022
[3] T. Cavaleri, P. Buscaglia, C. Caliri, E. Ferraris, M. Nervo, F.P. Romano, *Below the surface of the coffin lid of Neskhonsuennekhy in the Museo Egizio collection*, in X-Ray Spectrometry (2020) Special Issue article, https://doi.org/10.1002/xrs.3184 2020
[4] T. Cavaleri, S. Legnaioli, F. Lozar, C. Comina, F. Poole, C. Pelosi, A. Spoladore, D. Castelli, V. Palleschi, *A multi-analytical study of an ancient Egyptian limestone stela for knowledge and conservation purposes: recovering hieroglyphs and figurative details by image analysis*, Heritage 2021, 4(3), 1193-1207; https://doi.org/10.3390/heritage4030066 2021
[5] L. Es Sebar, L. Lombardo, P. Buscaglia, T. Cavaleri, A. Lo Giudice, A. Re, M. Borla, S. Aicardi, S. Grassini, *3D Multispectral Imaging for Cultural Heritage Preservation: The Case Study of a Wooden Sculpture of the Museo Egizio di Torino*, Heritage, 6, 2783–2795, 2023.
[6] L. Vigorelli, A. Re, L. Guidorzi, T. Cavaleri, P. Buscaglia, M. Nervo, F. Facchetti, M. Borla, S. Grassini, A. Lo Giudice, *X-ray imaging investigation and study on the gilding technique of an ancient Egyptian Taweret wooden statuette*, Journal of Imaging 2021, 7, 229. https://doi.org/10.3390/jimaging7110229, MDPI, 2021

[7] L. Vigorelli, A. Re, P. Buscaglia, N. Manfredda, M. Nervo, T. Cavaleri, P. Del Vesco, M. Borla, S. Grassini, L. Guidorzi, A. Lo Giudice, *Comparison of two ancient Egyptian Middle Kingdom statuettes from the Museo Egizio of Torino through computed tomographic measurements*, Journal of Archaeological Science: Reports, Volume 44, 2022, 103518, ISSN 2352-409X, https://doi.org/10.1016/j.jasrep.2022.103518, 2022
[8] L. Vigorelli, A. Re, L. Guidorzi, T. Cavaleri, P. Buscaglia, M. Nervo, P. Del Vesco, M. Borla, S. Grassini, A. Lo Giudice, *Multi-analytical approach for the study of an ancient Egyptian wooden statuette from the collection of Museo Egizio of Torino*, ACTA IMEKO ISSN: 2221-870X, March 2022, Volume 11, Number 1, pp. 1 – 10, 2022
[9] Colantonio, C.; Lanteri, L.; Ciccola, A.; Serafini, I.; Postorino, P.; Censorii, E.; Rotari, D.; Pelosi, C. *Imaging Diagnostics Coupled with Non-Invasive and Micro-Invasive Analyses for the Restoration of Ethnographic Artifacts from French Polynesia*, Heritage 5(1), 2022, 215–232. DOI:10.3390/heritage5010012
[10] Colantonio, C.; Clivet, L.; Laval, E.; Coquinot, Y.; Maury, C.; Melis, M.; Boust, C. *Integration of multispectral imaging, XRF mapping and Raman analysis for noninvasive study of illustrated manuscripts: the case study of 15th century Humay meets the Princess Humayun Persian masterpiece from Louvre Museum*, European Physical Journal Plus 136(9), 2021. DOI:10.1140/epjp/s13360-021-01909-8
[11] Ricci, M.; Laureti, S.; Malekmohammadi, H.; Sfarra, S.; Lanteri, L.; Colantonio, C.; Calabrò, G.; Pelosi, C. *Surface and interface investigation of a 15th-century wall painting using Multispectral Imaging and Pulse-Compression Infrared Thermography*, Coatings 11, 2021, 546. DOI:10.3390/coatings11050546
[12] Laureti, S.; Colantonio, C.; Burrascano, P.; Melis, M.; Calabrò, G.; Malekmohammadi, H.; Sfarra, S.; Ricci, M.; Pelosi C. *Development of integrated innovative techniques for painting diagnostics: the cases study of The Resurrection of Christ attributed to Andrea Mantegna and the Crucifixion of Viterbo*, Journal of Cultural Heritage 40, 2019, 1-16. DOI: 10.1016/j.culher.2019.05.005
[13] Romano, F.P. et al. (2017). *FF-XRF, XRD, and PIXE for the Nondestructive Investigation of Archaeological Pigments*. In: *Masini, N., Soldovieri, F. (eds) Sensing the Past. Geotechnologies and the Environment*, vol 16. Springer, Cham. https://doi.org/10.1007/978-3-319-50518-3_15
[14] Sarrazin, P., G. Chiari, and M. Gailhanou. *A portable non-invasive XRD-XRF instrument for the study of art objects*. Advances in X-ray analysis 52 (2008): 175-86.
[15] Delaney, John K., et al. "Integrated X-ray fluorescence and diffuse visible-to-near-infrared reflectance scanner for standoff elemental and molecular spectroscopic imaging of paints and works on paper." Heritage Science 6 (2018): 1-12.
[16] Emilio Catelli, Zelan Li, Giorgia Sciutto, Paolo Oliveri, Silvia Prati, Michele Occhipinti, Alessandro Tocchio, Roberto Alberti, Tommaso Frizzi, Cristina Malegori, Rocco Mazzeo, *Towards the non-destructive analysis of multilayered samples: A novel XRF-VNIR-SWIR hyperspectral imaging system combined with multiblock data processing*, *Analytica Chimica Acta*, Volume 1239, 2023, 340710, ISSN 0003-2670, https://doi.org/10.1016/j.aca.2022.340710.
[17] Augusto Pifferi, Gaetano Campi, Carmelo Giacovazzo, and Ettore Gobbic, *A New Portable XRD/XRF Instrument for Non-destructive Analysis*, Croat. Chem. Acta 82 (2) (2009) 449–454, ISSN-0011-1643, ISSN-1334-417X
[18] Hellen C. Santos, Tiago F. Silva, Alisson R. Leite, Renan F. Assis, Pedro H. O. V. Campos, Marcia A. Rizzutto, and Manfredo H. Tabacniks, *Characterization of a system that combines energy dispersive X-ray diffraction with X-ray fluorescence and its potential applications in archeometry*, Journal of Applied Physics 126, 044901 (2019) https://doi.org/10.1063/1.5108746
[19] Picollo, M.; Cucci, C.; Casini, A.; Stefani, L. *Hyper-Spectral Imaging Technique in the Cultural Heritage Field: New Possible Scenarios*. Sensors 2020, 20, 2843. https://doi.org/10.3390/s20102843
[20] Matthias Alfeld, José A.C. Broekaert, *Mobile depth profiling and sub-surface imaging techniques for historical paintings: A review*, Spectrochimica Acta Part B: Atomic Spectroscopy, Volume 88, 2013, pp. 211-230, ISSN 0584-8547, https://doi.org/10.1016/j.sab.2013.07.009.
[21] Romano, Francesco Paolo, Claudia Caliri, Paolo Nicotra, Sandra Di Martino, Lighea Pappalardo, Francesca Rizzo, and Hellen Cristine Santos. *Real-time elemental imaging of large-dimension paintings with*

a novel mobile macro X-ray fluorescence (MA-XRF) scanning technique. Journal of Analytical Atomic Spectrometry 32, no. 4 (2017): 773-781.
[22] M. Gargano, F. Cavaliere, D. Viganò, A. Galli, N. Ludwig, A new spherical scanning system for infrared reflectography of paintings, Infrared Physics & Technology, Volume 81, 2017, Pages 128-136, ISSN 1350-4495, https://doi.org/10.1016/j.infrared.2016.12.011.
[23] Silipigni, G., Burrascano, P., Hutchins, D. A., Laureti, S., Petrucci, R., Senni, L., & Ricci, M. (2017). *Optimization of the pulse-compression technique applied to the infrared thermography nondestructive evaluation. NDT & E International*, 87, 100-110.
[24] Laureti, S., Sfarra, S., Malekmohammadi, H., Burrascano, P., Hutchins, D. A., Senni, L., ... & Ricci, M. (2018). *The use of pulse-compression thermography for detecting defects in paintings*. Ndt & E International, 98, 147-154.
[25] Daffara, C.; Ambrosini, D.; Pezzati, L.; Marchioro, G. *Thermal Quasi-Reflectography (TQR): Current Research and Potential Applications*.; Pezzati, L., Targowski, P., Eds.; Munich, Germany, May 30 2013; p. 87900S.
[26] T. Cavaleri, P. Manchinu, B. Ventura, *Il restauro della Madonna della tenda: note sulla tecnica di esecuzione e sulla storia conservativa*, in Bava, A.; Villano, S. (eds.), Sulle tracce di Raffaello nelle collezioni sabaude; Editris, Torino, Italy, 2021, pp. 58-69.
[27] J. Sanyova, S. Cersoy, P. Richardin, O. Laprévote, P. Walter, A. Brunelle. Unexpected Materials in a Rembrandt Painting Characterized by High Spatial Resolution Cluster-TOF-SIMS Imaging, Anal. Chem. 2011, 83, 753–760.
[28] M. Noun, E. Van Elslande, D. Touboul, H. Glanville, S. Bucklow, P. Walter, A. Brunelle. High mass and spatial resolution mass spectrometry imaging of Nicolas Poussin painting cross section by cluster TOF-SIMS, J. Mass Spectrom. 2016, 51, 1196–1210.
[29] Križnar, Anabelle, Francisco J. Ager, Claudia Caliri, Francesco Paolo Romano, Miguel Ángel Respaldiza, María Auxiliadora Gómez-Morón, Lourdes Núñez, and Rocío Magdaleno. *Study of two large-dimension Murillo's paintings by means of macro X-ray fluorescence imaging, point X-ray fluorescence analysis, and stratigraphic studies.*" X-Ray Spectrometry 48, no. 5 (2019): 482-489.
[30] Nervo, Marco, Francesco P. Romano, Claudia Caliri, Anna Piccirillo, Paolo Triolo, Daniele Demonte, Alessandro Gatti, Eleonora Vergallo, Michela Cardinali, and Marianna Ferrero. "*Costruzione del viadotto": MA-XRF in the pictorial executive technique of Agostino Bosia*. X-Ray Spectrometry 50, no. 4 (2021): 253-262.
[31] T. Cavaleri, P. Buscaglia, S. Migliorini, M. Nervo, G. Piccablotto, A. Piccirillo, M. Pisani, D. Puglisi, D. Vaudan, M. Zucco. *Pictorial materials database: 1200 combinations of pigments, dyes, binders and varnishes designed as a tool for heritage science and conservation*. Appl. Phys. A 2017; 123, 419).
[32] Renè de la Rie E., Fluorescence of paint and varnish layers (Part I), Studies in Conservation n.27, pp. 1-7, 1982.
[33] Miliani, C., Romani, A., and Favaro, G. (1998). A spectrophotometric and fluorimetric study of some anthraquinoid and indigoid colorants used in artistic paintings. Journal of Spectrochimica Acta Part A, 54, pp. 581–588. https://doi.org/10.1016/S1386-1425(97)00240-0
[34] A. Pelagotti, L. Pezzati, N. Bevilacqua, V. Vascotto, V. Reillon, C. Daffara, A study of UV fluorescence emission of painting materials, in Art '05 8th International Conference on Non-Destructive Investigations and Microanalysis for the Diagnostics and Conservation of the Cultural and Environmental Heritage, A97, Lecce, 2005.
[35] T. Cavaleri, G. Fiocco, T. Rovetta, P. Dondi, M. Malagodi, M. Gulmini, A. Piccirillo, M. Pisani, M. Zucco, M. Gargano, A new imaging method of fluorescence induced by multispectral UV for studying historical musical instruments coatings, in Conservation 360°: UV-Vis Fluorescence imaging techniques, Ed. M. Picollo, M. Stols-Witlox & L. Fuster-López 2020
[36] M. Gulmini, A. Idone, E. Diana, D. Gastaldi, D. Vaudan, M. Aceto, Identification of dyestuffs in historical textiles: Strong and weak points of a non-invasive approach, Dyes and Pigments, Volume 98, Issue 1, 2013,

Pages 136-145, ISSN 0143-7208, https://doi.org/10.1016/j.dyepig.2013.02.010.
[37] Fiocco, G.; Rovetta, T.; Gulmini, M.; Piccirillo, A.; Canevari, C.; Licchelli, M.; Malagodi, M. Approaches for Detecting Madder Lake in Multi-Layered Coating Systems of Historical Bowed String Instruments. Coatings 2018, 8, 171. https://doi.org/10.3390/coatings8050171
[38] Fonseca, B., Schmidt Patterson, C., Ganio, M. et al. Seeing red: towards an improved protocol for the identification of madder- and cochineal-based pigments by fiber optics reflectance spectroscopy (FORS). Herit Sci 7, 92 (2019). https://doi.org/10.1186/s40494-019-0335-1
[39] Conti, C., Striova, J., Aliatis, I., Possenti, E., Massonnet, G., Muehlethaler, C., Poli, T., Positano, M., 2014. The detection of copper resinate pigment in works of art: contribution from Raman spectroscopy: Detection of copper resinate pigment in works of art. J. Raman Spectrosc. 45, 1186–1196. https://doi.org/10.1002/jrs.4455.
[40] Kühn, H., 2008. Verdigris and copper resinate, in artists' pigments. A handbook of their history and characteristics.
[41] Hermann Kühn, Verdigris and Copper Resinate, Studies in Conservation, Feb., 1970, Vol. 15, No. 1 (Feb., 1970), pp. 12-36.
[42] N. Eastaugh, V. Walsh, T. Chaplin, R. Siddall, Pigment compendium: a dictionary of historical pigments, BH Elsevier, Oxford, 2008, pp. 105 and pp. 103.
[43] E. Manzano, L.R. Rodriguez-Simón, N. Navas, R. Checa-Moreno, M. Romero-Gámez, L.F. Capitan-Vallvey, Study of the GC–MS determination of the palmitic–stearic acid ratio for the characterisation of drying oil in painting: La Encarnación by Alonso Cano as a case study, Talanta, Volume 84, Issue 4, 2011, Pages 1148-1154, ISSN 0039-9140, https://doi.org/10.1016/j.talanta.2011.03.012.
[44] Michael R. Schilling, Arlen Heginbotham, Henk van Keulen & Mike Szelewski (2016) Beyond the basics: A systematic approach for comprehensive analysis of organic materials in Asian lacquers, Studies in Conservation, 61:sup3, 3-27, DOI: 10.1080/00393630.2016.1230978
[45] A. Andreotti, I. Bonaduce, M.P. Colombini, G. Gautier, F. Modugno, E. Ribechini, Anal. Chem. 78 (2006) 4490.
[46] A. Piccirillo, D. Scalarone, O. Chiantore, J. Anal. Appl. Pyrol. 74 (2005) 33.
[47] D. Scalarone, M. Lazzari, O. Chiantore, J. Anal. Appl. Pyrol. 64 (2002) 345-361.
[48] V.P. Papageorgiou, M.N. Bakola-Christianopoulou, K.K. Apazidou, E.E. Psarros, J. Chromatogr. A, 769 (1997) 263–273.
[49] M.T. Doménech-Carbó, G. Bitossi, L. Osete-Cortina, D.J. Yusá-Marco, Study of ageing of ketone resins used as picture varnishes by pyrolysis–silylation–gas chromatography–mass spectrometry, J. Anal. Appl. Pyrolysis 85 (2009) 470–479.
[50] I. Bonaduce, M. P. Colombini, I. Degano, F. Di Girolamo, J. La Nasa, F. Modugno, S. Orsini. Mass spectrometric techniques for characterizing low-molecular-weight resins used as paint varnishes, Anal Bioanal Chem 405, 1047–1065 (2013).
[51] A. Asperger, W. Engewald, G. Fabian, J. Anal. Appl. Pyrolysis 52 (1999) 51-63.
[52] I. Bonaduce, M.P. Colombini, Characterisation of beeswax in works of art by gas chromatography–mass spectrometry and pyrolysis–gas chromatography–mass spectrometry procedures, Journal of Chromatography A, 1028 (2004) 297-306.

Acknowledgments

The authors would like to thank Annamaria Bava and Sofia Villano, Galleria Sabauda Musei Reali Torino, Turin, Italy, for promoting this study and authorizing using the images of the panel painting. Thanks also to Dario Vaudan and Simonetta Migliori, Laboratorio Analisi Scientifiche della Soprintendenza Regione Autonoma Valle d'Aosta, Italy, for their help collecting FORS data, and to the CCR colleagues Daniele Demonte, Alessandro Bovero, and Federico Di Iorio for technical photography. D. Scalarone acknowledges support from the Project CH4.0 under the MUR program "Dipartimenti di Eccellenza 2023-2027" (CUP:

D13C22003520001).